

DR. NOHA I ZIEDAN (Orcid ID : 0000-0002-9522-2188)

Received Date : 03-Sep-2016
Revised Date : 30-Nov-2016
Accepted Date : 19-Dec-2016
Article type : Research Article

Virtual screening, SAR and discovery of 5-(indole-3-yl)-2-[(2-nitrophenyl)amino] [1,3,4]-oxadiazole as a novel Bcl-2 inhibitor

Noha I. Ziedan^{1,2}, Rania Hamdy^{1,2}, Alessandra Cavaliere¹, Malamati Kourti^{1,3}, Filippo Prencipe¹, Andrea Brancale¹, Arwyn T. Jones¹, Andrew D. Westwell¹

¹School of Pharmacy and Pharmaceutical Sciences, Cardiff University, Redwood Building, King Edward VII Avenue, Cardiff, CF10 3NB, Wales, U.K.

²Faculty of Pharmacy, Zagazig University, Zagazig, 44516, Egypt

³Cardiff China Medical Research Collaborative, Cardiff University, Henry Wellcome Building, Heath Park Way, Cardiff, CF14 4XN

Corresponding author email id: nohazi@yahoo.com

Abstract

A new series of oxadiazoles were designed to act as inhibitors of the anti-apoptotic Bcl-2 protein. Virtual screening led to the discovery of new hits that interact with Bcl-2 at the BH3 binding pocket. Further study of the structure-activity relationship of the most active compound of the first series, compound **1**, led to the discovery of a novel oxadiazole analogue, compound **16j**, that was a more potent small molecule inhibitor of Bcl-2. **16j** had good *in vitro* inhibitory activity with sub-micromolar IC₅₀ values in a metastatic human breast cancer cell line (MDA-MB-231) and a human cervical cancer cell line (HeLa). The antitumour effect of **16j** is concomitant with its ability to bind to Bcl-2 protein as shown by an enzyme linked immunosorbent assay (IC₅₀ = 4.27 μM). Compound **16j** has a great potential to develop into highly active anticancer agent.

Introduction

Apoptosis is a complex and highly orchestrated cellular process, and disruption of the balance between induction and inhibition of apoptosis play key roles in progression of a number of diseases. A well-studied example of this is the identification and study of apoptosis inhibition as a key hallmark of cancer. (1) The Bcl-2 family is a related group of regulatory proteins that play critical roles in

This article has been accepted for publication and undergone full peer review but has not been through the copyediting, typesetting, pagination and proofreading process, which may lead to differences between this version and the Version of Record. Please cite this article as doi: 10.1111/cbdd.12936

This article is protected by copyright. All rights reserved.

cellular apoptosis, either by inducing (pro-apoptotic) or inhibiting (anti-apoptotic) apoptosis. (2) Bcl-2 itself, the prototypical member of this family, is an important anti-apoptotic protein that has been the target of a number of drug discovery and development efforts over recent years. (3)

Inhibition of anti-apoptotic family members such as Bcl-2 itself has become an attractive therapeutic strategy as Bcl-2 inhibition should lead to a selective (non-genotoxic) pro-apoptotic cascade from which cancer cells cannot easily recover. A number of small molecule Bcl-2 inhibitors have been developed that have progressed to clinical development; prominent among these are the BH3-mimetic structural analogues ABT-737 and ABT-263 (Navitoclax, Figure 1), which also inhibit Bcl-2 family members Bcl-X_L and Bcl-w and are currently under investigation in a number of combination studies. (4) Obatoclax mesylate (Figure 1) is a pan-Bcl-2 inhibitor under clinical investigation in the leukemia and lymphoma field. (5) Venetoclax (Figure 1, formerly known as ABT-199), a selective and orally bioavailable Bcl-2 inhibitor structurally related to ABT-737/263, is progressing with FDA “Breakthrough Designation” into Phase III development in acute myelogenous leukaemia (AML) and chronic myelogenous leukaemia (CML) following encouraging Phase II data in these settings. (6) Our own previous investigations into the discovery of new indole-based Bcl-2-inhibitory pro-apoptotic agents (7) has included the identification of antitumour indolyl-oxadiazoles, (8) indolyl-isoxazoles (9) and indolyl-triazolamines. (10) In this paper we report the computational design, virtual screening, analogue synthesis and *in vitro* evaluation of new Bcl-2 inhibitory agents based on an indolylamino-oxadiazole scaffold.

Results and discussion

Virtual screening and initial *in vitro* biological evaluation

Our virtual screening began with the construction of a 3D pharmacophore model for Bcl-2 inhibitor design within the Molecular Operating Environment from Chemical Computing Group (11). A database of 12 reported active compounds was created (1YSW (12), 1YSI (12), 2O2F (12), ABT-737 (13), TW-37 (14), TM-1206 (15), acylpyrogallol (15), YC137 (16), BHI-1 (17), BHI-2 (17), HA 14-1 (18) and NSC365400 (19)). Three out of the twelve compounds were derived directly from their 3D NMR structure in complex with Bcl-2 protein (PDB code: 1YSW, 1SYI and 2O2F). These latter structures were used to create the 3D model, by refining the existing alignment of their crystallized conformation followed by flexible alignment of another active compound (14) (TW-37) with the fixed aligned structures.

Taking into account the four main interactions previously reported (14) that are needed for the stabilization of the complex between pro-apoptotic Bim and anti-apoptotic Bcl-2, a seven feature 3D pharmacophore model was built (Figure 2). The model was tested against the created library. Eleven out of the 12 compounds matched the query with F1 and F4 as essential features, at least one of F6 and F7, at least one of F3 and F5 and enabling partial match to a minimum of five features. F1 represents a hydrogen bond acceptor mimicking Asn102 of Bim BH3; F3 and F5 are two possible positions for hydrophobic interaction mimicking Phe101 of Bim peptide; and F6 and F7 are possible hydrophobic interactions mimicking Leu94 of Bim peptide.

In an effort to discover novel inhibitors of anti-apoptotic Bcl-2, a drug-like subset database from the ZINC database (<http://zinc.docking.org/subset1/3/index.html>) was downloaded and filtered using the ADME filter within MOE. As drug-like molecules, most molecules had an acceptable ADME profile, so the reduction in the size of the database was neglected. The starting number of virtual molecules was 530,000 compounds. Conformational import with strain limit of 4 Kcal/mol of all molecules was

run to take flexibility into account. The database was tested against the built 3D pharmacophore model (F1 and F4 as essential features, at least one of F6 and F7, at least one of F3 and F5 and enabling partial match to a minimum of five features), which reduced the number of molecules to 15,880. The NMR structure of Bcl-2 co-crystallized with a ligand related to the lead Bcl-2 inhibitory agent ABT-737 (PDB code: 1YSW) was retrieved from the Protein Data Bank (PDB) for docking of successful molecules into the active site using FlexX.(20) After ranking of the docked molecules and visual inspection of the binding modes of the highest scoring molecules, 259 molecules were selected. Of these, 15 compounds were chosen for synthesis and testing as Bcl-2 inhibitors based on considerations of interaction score and binding interactions.

All 15 compounds (shown in Figure 3) were tested for their inhibitory activity *in vitro* on two human cancer cell lines (cervical HeLa and breast MDA-MB-231) using the colorimetric MTT cell proliferation assay (72 h) to assess viability (Table 1). These two cancer cell lines are well established in our laboratory for the initial screening for growth inhibitory activity of newly synthesized compounds. The MDA-MB-231 breast cancer cell line is known to express Bcl-2 and previous studies have shown down-regulation of Bcl-2 in these cells by Western blot analysis following inhibitor treatment. (21) Stable expression of Bcl-2 in the HeLa cell line is also well known. (22) The most active compounds, based on viability assays, from this initial series (compounds **1**, **2**, **6** and **8**) were chosen to test their competitive binding for Bcl-2 protein using the ELISA assay (Table 2), based on a previously described for assessing Bcl-2 binding affinity (15) . The pro-apoptotic Bcl2-inhibitory natural product gossypol, an agent under clinical investigation in cancer (23), was used as a positive control in these experiments.

Some of the tested compounds showed good to moderate anti-proliferative activity with IC₅₀ values in the low micromolar range. Of those, compound **1** and **8** had the most potent activity. Compound **1** was 3-fold more active than gossypol against the MDA-MB-231 cell line and 10-fold more active against the HeLa cell line. As the most active compound within this series, we were interested to know whether compound **1** possessed growth inhibitory activity against the normal breast epithelial cell line, MCF-10A (under the same test conditions as for the human cancer cell lines). Compound **1** was found to have an IC₅₀ value (MCF-10A) of 2.51 ± 0.29 μM, a slightly higher IC₅₀ value compared to that observed in the cancer cell lines and suggestive of selective anticancer activity. On the other hand, compound **8** showed similar activity to gossypol against both cancer cell lines. However, none of the tested compounds had better competitive binding for Bcl-2 than gossypol (Table 2). The indole-based oxadiazole thiols (compounds **1**, **2** and **6**, Fig 3) bind moderately to Bcl-2 with IC₅₀ values ranging between 10 and 17 μM. Compound **8** did not show any binding activity to Bcl-2 as shown in the ELISA assay. The ease of synthesis of these compounds and their relative low molecular weight made them attractive leads for further optimization toward development of a novel class of Bcl-2 inhibitors.

Optimization and design of novel Bcl-2 inhibitors

The structure of the most active hit was modified in an attempt to further investigate the involvement of each part of the structure in the interaction with Bcl-2 with the aim of designing novel and easily accessible Bcl-2 inhibitors. The core structure of indolyl oxadiazoles represented by **1** was divided conceptually into four main regions as shown in Figure 4.

In part A, the original 3-indolyl in our most active hit **1** was replaced by a naphthoxymethyl, phenoxyethyl or indolylmethyl group to better understand the importance of the hydrophobic ring

size in relation to interaction at the hydrophobic groove. For part B the oxadiazole ring was replaced with the bioisosteric 1-aminotriazole to explore the importance of this ring in the activity of this series of compounds. Moreover, the opening of the ring was also explored (compound **17**). Replacement of the ring with an open chain group was performed to study the extent of interaction of the 1,3,4-oxadiazole ring with Bcl-2 and try to obtain structurally simplified compounds. The distance between the 5-membered ring and the terminal phenyl group was varied to explore the best distance that placed these two rings in their optimum position inside the hydrophobic binding groove in Bcl-2; part C. Part D was modified by using different substitutions in the terminal phenyl group. In addition to the changes in the above four parts of the structure, the spatial arrangement of the groups around the 5-membered heterocyclic ring was also studied (compounds **18a-d**). Vicinal substituted rings were designed to study the spatial positioning of the substituted groups around the central five-membered heterocycle. The chemical structures of newly designed compounds arising from consideration of structure-activity relationship around compound **1** are shown in Figure 5.

Chemical Synthesis

The general strategy for synthesis of all designed compounds is shown in Schemes 1-3. The intermediate 1,2,4-oxadiazole derivatives were obtained in two steps starting from the corresponding ester (**19a,b**) via conversion to hydrazide (**20a,b**) using hydrazine monohydrate followed by cyclization into 1,3,4-oxadiazole-2(3H)-thione (**21a,b**) using carbon disulfide. Refluxing oxadiazolethiol **21b** with hydrazine monohydrate afforded the 4-triazolamine **22**. S-alkylation with different chloracetamides gave the corresponding thioethers (compounds **16a-c, h, i**; Scheme 1). Reduction of the nitro derivatives **1,3** with Fe in HCl gave the amino derivative (compounds **16d,e**; Scheme 2). Coupling of the 4-amino derivative **16d** with different acyl chlorides in THF under basic conditions furnished the corresponding 4-amides (compounds **16f,g**; Scheme 2). The thiosemicarbazide (ring opened analog) was prepared by reacting **20b** with 2-nitrophenyl isothiocyanate (compound **17**; Scheme 3). Thiosemicarbazides (**23a-e**) were either cyclized into 1,3,4-oxadiazole-5-amine by reaction with 1,3-dibromo-5,5-dimethylhydantoin in acetonitrile (compounds **16j-m**; Scheme 3), or to 4-substituted 1,2,4-triazolethiol (**24a-c**) by refluxing in 2N NaOH or saturated sodium carbonate **24a-c**. S-alkylation of **24a,b** gave the corresponding thioether (compounds **16n,o**). **24a** was reduced into the amino derivative with Fe/HCl, followed by N-acylation with different acylchlorides to give **18a,c,d**. Demethylation of the dimethoxyphenyl derivative **18a** with boron tribromide afforded the corresponding dihydroxyphenyl compound **18b**.

Biological results and discussion

In vitro anti-proliferative activities

Table 3 summarizes the growth inhibitory effects of newly synthesized compounds **16a-o, 17, 18a-d**, the previous hit compound **1** and gossypol as a reference compound against both breast MDA-MB-231 and cervical HeLa human cancer cell lines. Oxadiazolthio derivatives showed the best activity, where, replacement with triazolamine **16h,i** showed complete loss of activity. The connector between the oxadiazole and the phenyl also affected the potency of the compounds. The 4-atom connector was much better than the 2-atom connector. Compounds **1** and **16a** with 4 atom connector (-S-CH₂-CO-NH-) had much better inhibitory activity than their methylthio (2-atom connector) counterparts; **16b,c**. The IC₅₀ of **1** and **16a** on MDA-MB-231 cells were reduced from 1.72 and 10.22 μM to 0.996 and 24.4 μM for their methylthio counterpart **16c** and **16d** respectively. The amino derivative **16j**, however, showed a 2-fold increase in the potency compared to the lead compound **1** with IC₅₀ of 0.91 and 0.25 against MDA-MB-231 and HeLa respectively. As previously for compound **1**, we studied the anti-proliferative activity in a normal breast epithelial cell line, MCF-10A. The less potent IC₅₀

value of $3.16 \pm 1.24 \mu\text{M}$ was indicative of selective anticancer activity within the cancer cell lines compared to normal control. Increasing the connection between the oxadiazole and the indole with a methylene group reduced the activity, as shown for compounds **16k** and **16l**. The type of the substituent on the phenyl ring also affected the potency, with the nitro group tending to have the best inhibitory activity. Replacement of the nitro group in **1** with an amino group in **16d** abolished the growth inhibitory effect. However, more extended substituent at the 4-position improved the potency, where, **16f** with an acetylamino group had an IC_{50} of $16.45 \mu\text{M}$ on MDA-MB-231, while **16g** with a phenoxyacetamido group was almost 2-fold more active than **16h** with an IC_{50} of $9.9 \mu\text{M}$ on MDA-MB-231. Variation in the type of 5-substituent of the 1,3,4-oxadiazole ring affected the potency. The 3-indolyl derivatives had the best activity. Replacement with naphthyloxymethyl group in **16a** showed some activity with IC_{50} in low micromolar range in comparison to $37.97 \mu\text{M}$ in its 3-indolyl counterpart **3** in MDA-MB-231 cells (Table 1). Opening of the 5-membered ring (compound **17**) completely abolished the activity. Compounds **18a-d** with vicinal substitution on the 5-membered ring had some potency, but still much less active than the lead compound **1**.

Competitive binding to anti-apoptotic Bcl-2 protein

To investigate whether the anti-proliferative activity of the most active compound was derived from inhibition of the anti-apoptotic Bcl-2 protein, cellular active compounds **16g**, **16j** and **18d** were tested for their competitive binding for Bcl-2 using ELISA. Table 4 summarizes the IC_{50} values of these compounds in comparison to the lead compound **1**.

The oxadiazole-5-amine **16j** had the best affinity for Bcl-2 with an ELISA value of IC_{50} of $4.27 \mu\text{M}$; almost half the affinity of gossypol. The growth inhibitory effect of **16j** coincides with its ability to bind to Bcl-2 as it had the most potent *in vitro* inhibitory effect on both HeLa and MDA-MB-231 cell lines. Indole based oxadiazole thiols (**1** and **16g**) had moderate binding affinity to Bcl-2 with IC_{50} around $16 \mu\text{M}$. Compound **18d** with vicinal substituted triazole also showed moderate affinity for Bcl-2 with an IC_{50} of $10.66 \mu\text{M}$.

Molecular modeling

Molecular modeling studies were used to further our understanding of the structure-activity relationships of the compounds discussed above. The NMR structure of Bcl-2 co-crystallized with a ligand (PDB code: 1YSW) was used to define the active site. The BH3 binding groove on Bcl-2 is quite a large binding pocket can be viewed as composed of two large hydrophobic grooves (site 1 and site 2) and a shallow linker (aromatic ridge) (L) in between the two sites (figure 7)

All the synthesized compounds were subjected to a docking study to explore their affinity and binding mode to Bcl-2. The aim of the work was to rationalize the obtained biological data and explain the possible interactions that might take place between the novel compounds and anti-apoptotic Bcl-2 protein in comparison to crystallized ligand in order to optimize potent activity and selectivity.

Figure 7 shows the docking of **16j** with 3-indolyl (panel A and B) and **16m** with 3-indolylmethyl counterpart (C and D). **16j** with 3-indolyl substituent directly attached to the oxadiazole ring shows deep insertion of the 2-nitrophenyl group ring at site 2 with complete overlapping with the active ligand. The 3-indolyl group occupies the shallow linker site with optimized arene-cation interaction with Arg143. For **16m**, the presence of the methylene connector between the 3-indolyl and the oxadiazole made different interaction mode with Bcl-2 with the 3-indolylmethyl group less deeply inserted at the hydrophobic site 1 and the substituted phenyl group at the shallow linker with no interaction with Arg143.

Structure-activity relationship

Based on the cytotoxic profiles and Bcl-2 binding affinity of the designed compounds **16a-o**, **17** and **18a-d**, the following structural features were found to correlate to the activity.

Part A of the lead **1** (Figure 4) is that part which plays a role in the hydrophobic interaction at hydrophobic groves (site 2) of Bcl-2 mimicking Leu94 of Bim peptide. Bulky group showed better interaction. The docking showed deeper insertion into site 2 thus better hydrophobic interaction.

Part (B) is mostly located within the linker L and it could play a role in the interaction with Bcl-2 by forming hydrogen bonding with Gly142 or Arg143 mimicking Asn102 or Asp99 in Bim. Both 1,3,4-oxadiazole and 4-amino-1,2,4-triazole were investigated and only the oxadiazole ring showed activity. 4-Amino-1,2,4-triazole completely abolished the activity. Also, ring opening (compound **17**) completely eliminated the activity

Part (C) is located in the shallow linker L and it plays a role in positioning part (D) in the hydrophobic groove site 1. For the active oxadiazole derivatives, 4-Atom connectors optimize the position of part (D) into site 1 and give better inhibitory activity. 2-atom connectors have very weak inhibitory activity probably due to the inadequate insertion of part (D) into the hydrophobic groove site 1.

Part (D) is that part of the molecule that mostly occupies (site 1) in Bcl-2 mimicking Phe101 of the Bim peptide. Based on the biological results, both the site of substitution and its nature affect the activity. 4-Substituted phenyl generally gave the best results, where 4-NO₂ Ph was better than 2-NO₂. Also, smaller substituents were less active, where; the smaller F and NH₂ groups had less activity compared to larger electron-withdrawing groups like NO₂. Moreover, extending the substitution at the para position of the phenyl ring could enhance the binding and gave better activity, where, the more extended the substituent, the deeper its insertion into (site 1) making use of the hydrophobic interaction at this groove which in turn enhances the activity. 2-Methylphenoxyacetamide (**16g**) was more active than acetamide (**16f**), which in turn was better than NH₂ (**16d**).

Both vicinal and 1,3-disubstituted rings showed activity as Bcl-2 inhibitors. However, vicinal arrangement of the groups needed more extended substitution to show activity, where, the more extended the group, the more it is inserted into the hydrophobic groove (site 1) and the better is the activity. Also, the presence of more polar groups like hydroxyl (compound **18b**) reduced the activity probably due to the less hydrophobic interaction at site 1. So, for vicinal substituted rings, the more extended and more hydrophobic the group, the better is the anti-proliferative activity of the compound (**18d** compared to **18a**).

Conclusion

In summary, the design of novel non-peptidic molecules that act as Bcl-2 inhibitors began with virtual screening. The NMR structure of Bcl-2 co-crystallized with a peptide ligand was used for definition of the active site. A ligand-based 3D pharmacophore was created and over 500,000 compounds were tested against the model followed by docking and visual inspection which eventually led to the discovery of 15 hits as potential Bcl-2 inhibitors. Biological evaluation of the chosen hits led to the discovery of 3,5-disubstituted 1,3,4-oxadiazole (compound **1**) with moderate Bcl-2 inhibitory activity and a good cell inhibitory activity with IC₅₀ values in the submicromolar range. Compound **1** was modified at four different sites to investigate the structure-activity relationship of the 3,5-disubstituted 1,3,4-oxadiazoles with respects to: the C3-substituent, the five membered ring, the length of the connector at the C5 and the aromatic substitution at C5, in addition to the special arrangement of the groups around the 5 membered core. The study led to the discovery of compound **16j** with the best activity being almost 20-fold more active than gossypol in growth inhibitory assays in the cell lines tested and only 2-fold less active than gossypol as Bcl-2 inhibitor according to binding assays.

Compound **16j** represents a new class of small molecule inhibitors targeting the anti-apoptotic Bcl-2 proteins. Further molecular modelling and molecular dynamic studies could give more insight into the molecular interactions between **16j** and Bcl-2 which can lead to a design of more active compounds and translational progress.

Acknowledgements

We acknowledge the Egyptian Government for the award of a PhD student (to NIZ), and for the award of a Channel Scheme PhD Scholarship (to RH). We thank the EPSRC National Mass Spectrometry Facility (Swansea, U.K.) for assistance with accurate mass determinations.

References

1. Hanahan D, Weinberg RA (2011) Hallmarks of cancer: the next generation. *Cell*; **144**: 646-74.
2. Siddiqui WA, Ahad A Fau - Ahsan H, Ahsan H (2015) The mystery of BCL2 family: Bcl-2 proteins and apoptosis: an update. *Archives of toxicology*; **89**: 289-317.
3. Hata AN, Engelman JA, Faber AC (2015) The BCL2 Family: Key Mediators of the Apoptotic Response to Targeted Anticancer Therapeutics. *Cancer Discovery*; **5**: 475-87.
4. Hann CL, Daniel VC, Sugar EA, Dobromilskaya I, Murphy SC, Cope L, et al. (2008) Therapeutic efficacy of ABT-737, a selective inhibitor of BCL-2, in small cell lung cancer. *Cancer Res*; **68**: 2321-8.
5. Nguyen M, Marcellus RC, Roulston A, Watson M, Serfass L, Murthy Madiraju SR, et al. (2007) Small molecule obatoclax (GX15-070) antagonizes MCL-1 and overcomes MCL-1-mediated resistance to apoptosis. *Proc Natl Acad Sci U S A*; **104**: 19512-7.
6. Pietarinen PO, Pemovska T, Kontro M, Yadav B, Mpindi JP, Andersson EI, et al. (2015) Novel drug candidates for blast phase chronic myeloid leukemia from high-throughput drug sensitivity and resistance testing. *Blood Cancer J*; **5**: e309.
7. Ziedan NI, Kadri H, Westwell AD (2008) The development of pro-apoptotic cancer therapeutics. *Mini Rev Med Chem*; **8**: 711-8.
8. Ziedan NI, Stefanelli F, Fogli S, Westwell AD (2010) Design, synthesis and pro-apoptotic antitumour properties of indole-based 3,5-disubstituted oxadiazoles. *Eur J Med Chem*; **45**: 4523-30.
9. Md Tohid SF, Ziedan NI, Stefanelli F, Fogli S, Westwell AD (2012) Synthesis and evaluation of indole-containing 3,5-diarylisoxazoles as potential pro-apoptotic antitumour agents. *Eur J Med Chem*; **56**: 263-70.
10. Hamdy R, Ziedan N, Ali S, El-Sadek M, Lashin E, Brancale A, et al. (2013) Synthesis and evaluation of 3-(benzylthio)-5-(1H-indol-3-yl)-1,2,4-triazol-4-amines as Bcl-2 inhibitory anticancer agents. *Bioorg Med Chem Lett*; **23**: 2391-4.
11. Inc. CCG. (2010) Molecular Operating Environment (MOE). *Molecular Operating Environment (MOE)*. Montreal, QC, Canada, H3A 2R7.
12. Bruncko M, Oost TK, Belli BA, Ding H, Joseph MK, Kunzer A, et al. (2007) Studies leading to

potent, dual inhibitors of Bcl-2 and Bcl-xL. *J Med Chem*; **50**: 641-62.

13. Oltersdorf T, Elmore SW, Shoemaker AR, Armstrong RC, Augeri DJ, Belli BA, et al. (2005) An inhibitor of Bcl-2 family proteins induces regression of solid tumours. *Nature*; **435**: 677-81.

14. Wang G, Nikolovska-Coleska Z, Yang CY, Wang R, Tang G, Guo J, et al. (2006) Structure-based design of potent small-molecule inhibitors of anti-apoptotic Bcl-2 proteins. *J Med Chem*; **49**: 6139-42.

15. Tang G, Nikolovska-Coleska Z, Qiu S, Yang CY, Guo J, Wang S (2008) Acylpyrogallols as inhibitors of antiapoptotic Bcl-2 proteins. *J Med Chem*; **51**: 717-20.

16. Real PJ, Cao Y, Wang R, Nikolovska-Coleska Z, Sanz-Ortiz J, Wang S, et al. (2004) Breast cancer cells can evade apoptosis-mediated selective killing by a novel small molecule inhibitor of Bcl-2. *Cancer Res*; **64**: 7947-53.

17. Degterev A, Lugovskoy A, Cardone M, Mulley B, Wagner G, Mitchison T, et al. (2001) Identification of small-molecule inhibitors of interaction between the BH3 domain and Bcl-xL. *Nat Cell Biol*; **3**: 173-82.

18. Wang JL, Liu D, Zhang ZJ, Shan S, Han X, Srinivasula SM, et al. (2000) Structure-based discovery of an organic compound that binds Bcl-2 protein and induces apoptosis of tumor cells. *Proc Natl Acad Sci U S A*; **97**: 7124-9.

19. Enyedy IJ, Ling Y, Nacro K, Tomita Y, Wu X, Cao Y, et al. (2001) Discovery of small-molecule inhibitors of Bcl-2 through structure-based computer screening. *J Med Chem*; **44**: 4313-24.

20. www.biosolveit.de/FlexX. (2016) FlexX. *FlexX*.

21. Li Y, Upadhyay S, Bhuiyan M, Sarkar FH (1999) Induction of apoptosis in breast cancer cells MDA-MB-231 by genistein. *Oncogene*; **18**: 3166-72.

22. Elliott MJ, Stribinskiene L, Lock RB (1998) Expression of Bcl-2 in human epithelial tumor (HeLa) cells enhances clonogenic survival following exposure to 5-fluoro-2'-deoxyuridine or staurosporine, but not following exposure to etoposide or doxorubicin. *Cancer Chemother Pharmacol*; **41**: 457-63.

23. Gao P, Bauvy C, Souquère S, Tonelli G, Liu L, Zhu Y, et al. (2010) The Bcl-2 Homology Domain 3 Mimetic Gossypol Induces Both Beclin 1-dependent and Beclin 1-independent Cytoprotective Autophagy in Cancer Cells. *Journal of Biological Chemistry*; **285**: 25570-81.

Appendix S1

List of Bcl-2 inhibitors used in creating pharmacophore model. Synthetic schemes for all virtual screening chosen hits. All experimental data (detailed chemical synthesis and structure elucidation, biological assays and docking).

Figures legend:

Figure 1: Bcl-2 inhibitory clinical candidates.

Figure 2. Pharmacophore model. The pharmacophore with seven features are color coded as follows: H-bond acceptors as blue and hydrophobic aromatic regions as green.

Figure 3. Structures of selected virtual hit compounds.

Figure 4. Sub-division of the constituent components of the virtual hit indolyl-oxadiazole scaffold.

Figure 5. Structures of all newly designed compounds derived from original hit compound **1**.

Figure 6. (A, left panel) Interactions between pro-apoptotic Bim BH3 peptide and Bcl-2. Bim appears in red, Bcl-2 in green and small molecule inhibitor in yellow. Interaction analysis shows a hydrogen bonding network between residues Asn102 and Asp99 in Bim and Gly142 and Arg143 in Bcl-2. Three different hydrophobic interactions, where the residues Phe101 and Leu94 in Bim BH3 peptide seem to insert into the hydrophobic grooves 1 and 2 respectively of Bcl-2, and a hydrophobic contact between Ile97 in Bim and Bcl-2 at the shallow linker L can be observed. (B, right panel) The active site of Bcl-2 using 1YSW to define key sites of interaction and their stereoelectronic features.

Figure 7: Docking and ligand interaction of two designed compounds in the BH3 binding pocket of Bcl-2. Compounds appear in yellow, active ligand in green, Bcl-2 residues in red and the surface pocket in grey. (A) **16j**; (B) ligand interaction of **16j**; (C) **16m**; (D) ligand interaction of **16m**

Schemes list

- Scheme 1
- Scheme 2
- Scheme 3

Tables legend

Table 1: *In vitro* anti-proliferative effect of chosen virtual hit compounds against MDA-MB-321 and HeLa cancer cell lines using the MTT assay.

Table 2: The IC₅₀ of different compounds in Bcl-2 ELISA binding assays

Table 3: *In vitro* anti-proliferative effect of designed compounds against MDA-MB-231 and HeLa cancer cell lines using MTT assay

Table 4: IC₅₀ of active compounds using a Bcl-2 binding ELISA

Table 1: *In vitro* anti-proliferative effect of chosen virtual hit compounds against MDA-MB-321 and HeLa cancer cell lines using the MTT assay.

Compound No.	IC ₅₀ μM ^a	
	MDA-MB-231	HeLa
Gossypol	5.5 ± 0.34	4.43 ± 0.54
1	1.72 ± 0.59	0.4 ± 0.21
2	20.83 ± 1.2	42.09 ± 1.5
3	37.97 ± 2.3	75.42 ± 1.5
4	34.35 ± 1.3	>100
5	8.67 ± 0.94	20.89 ± 0.76
6	28.17 ± 1.6	6.4 ± 0.97
7	>100	>100
8	4.9 ± 0.32	6.4 ± 0.75
9	17.4 ± 1.7	5.9 ± 0.65
10	>100	20.36 ± 0.69
11	>100	42.09 ± 1.9
12	>100	19.04 ± 2.1
13	>100	>100
14	>100	>100
15	9.04 ± 0.78	ND ^b

^a Values are mean ± SD of three independent experiments

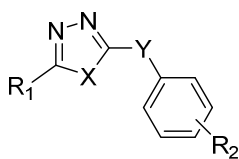
^b ND: Not determined

Table 2: The IC₅₀ of different compounds in Bcl-2 ELISA binding assays

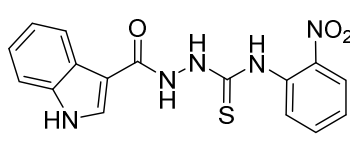
Compound No	IC ₅₀ μM ^a ELISA
Gossypol	2.11 ± 0.56
1	16.17 ± 0.97
2	10.25 ± 0.79
6	17.18 ± 1.02
8	>100

^a Values are mean ± SD of three independent experiments

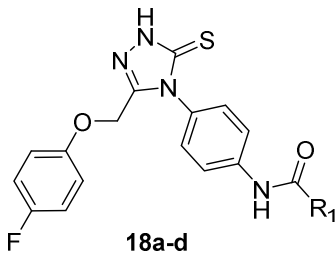
Table 3: *In vitro* anti-proliferative effect of designed compounds against MDA-MB-231 and HeLa cancer cell lines using MTT assay



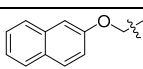
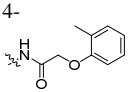
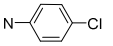
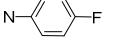
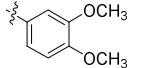
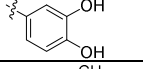
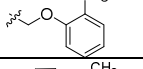
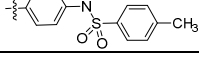
1, 16a-o



17



18a-d

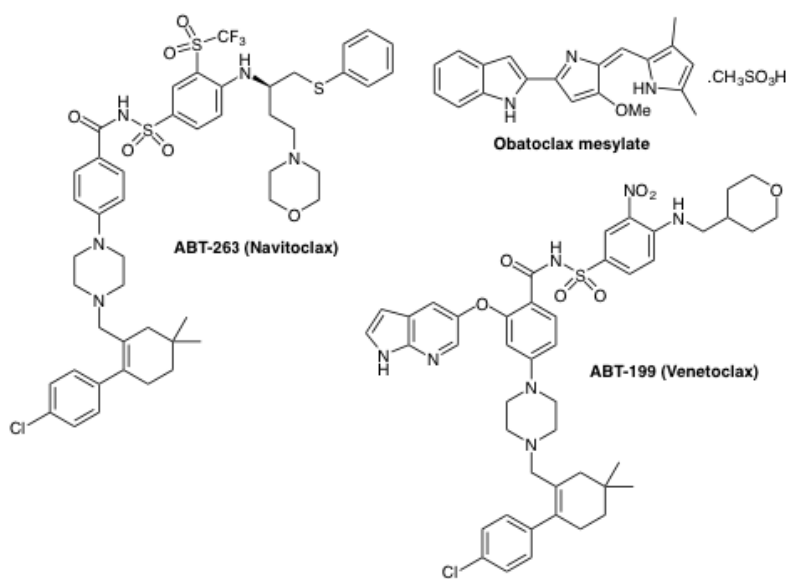
Compound No	R ₁	X	Y	R ₂	IC ₅₀ μM ^a	
					MDA-MB-231	HeLa
1	3-indolyl	O	-S-CH ₂ -CO-NH	4-NO ₂	1.72 ± 0.59	0.4 ± 0.21
16a		O	-S-CH ₂ -CO-NH	2-NO ₂	10.22 ± 0.58	16.14 ± 0.69
16b	3-indolyl	O	-S-CH ₂	3-NO ₂	99.64 ± 1.2	>100
16c	3-indolyl	O	-S-CH ₂	4-NO ₂	24.42 ± 2.3	>100
16d	3-indolyl	O	-S-CH ₂ -CO-NH	4-NH ₂	>100	>100
16e	3-indolyl	O	-S-CH ₂ -CO-NH	2-NH ₂	>100	>100
16f	3-indolyl	O	-S-CH ₂ -CO-NH	4-NHCOCH ₃	16.45 ± 2.5	32.70 ± 3.1
16g	3-indolyl	O	-S-CH ₂ -CO-NH		9.91 ± 0.54	8.6 ± 0.32
16h	3-indolyl	N-NH ₂	-S-CH ₂ -CO-NH	4-NO ₂	>100	>100
16i	3-indolyl	N-NH ₂	-S-CH ₂ -CO-NH	2-NO ₂	>100	>100
16j	3-indolyl	O	-NH	2-NO ₂	0.91 ± 0.21	0.25 ± 0.11
16k	3-indolylmethyl	O	-NH	3-Cl	67 ± 0.65	45 ± 0.25
16l	3-indolylmethyl	O	-NH	3,4-di Cl	78 ± 0.55	36.3 ± 0.81
16m	3-indolylmethyl	O	-NH	4-F	39 ± 0.69	33.28 ± 1.11
16n	3-indolylmethyl		-S-CH ₂ -CO-NH	3,4-di Cl	27 ± 0.15	31.17 ± 0.35
16o	3-indolylmethyl		-S-CH ₂ -CO-NH	3-NO ₂	38.2 ± 0.75	57.3 ± 0.51
17	-	-	-	-	>100	>100
18a		-	-	-	35.14 ± 1.6	73.25 ± 1.9
18b		-	-	-	83.38 ± 2.4	>100
18c		-	-	-	57.29 ± 3.1	77.8 ± 2.7
18d		-	-	-	16.68 ± 1.05	39.97 ± 1.2

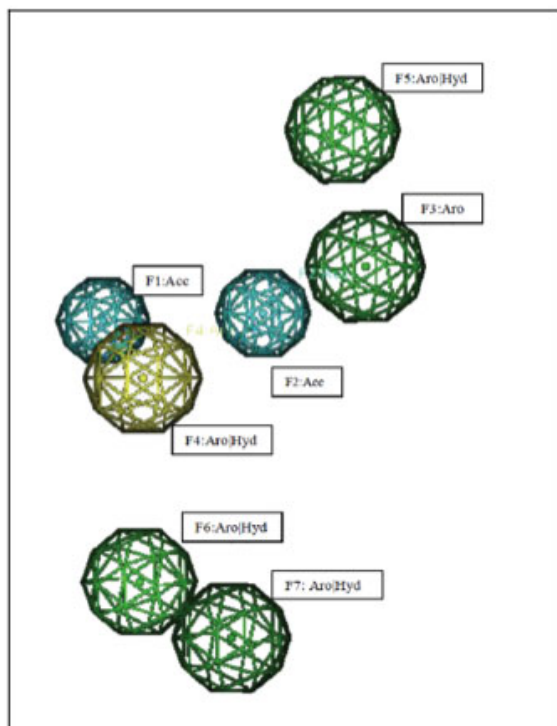
^a Values are mean \pm SD of three experiments

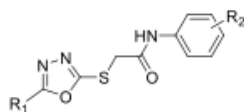
Table 4: IC₅₀ of active compounds using a Bcl-2 binding ELISA

Compound No	ELISA IC ₅₀ μ M ^a
1	16.17 \pm 0.97
16g	16.96 \pm 1.06
16j	4.27 \pm 0.34
18d	10.66 \pm 0.94

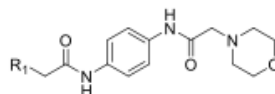
^a Values are mean \pm SD of three experiments



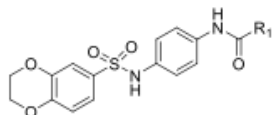




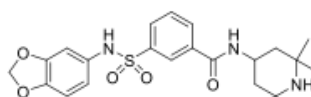
- 1; R₁ = 3-indolyl, R₂ = 4-NO₂
 2; R₁ = 3-indolyl, R₂ = 3-NO₂
 3; R₁ = 3-indolyl, R₂ = 2-NO₂
 4; R₁ = 3-indolyl, R₂ = 2-F
 5; R₁ = 3-indolyl, R₂ = 3-Br
 6; R₁ = 5-F-indol-2-yl, R₂ = 4-NO₂
 7; R₁ = 4-F-phenoxyethyl, R₂ = 3-Cl, 4-F



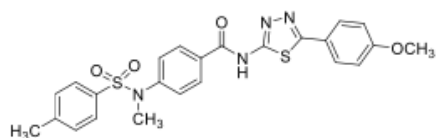
- 8; R₁ = 2-Cl Ph
 9; R₁ = 2-naphthyl
 10; R₁ = 2,5-diCl phenoxy
 11; R₁ = 4-Br phenylthio



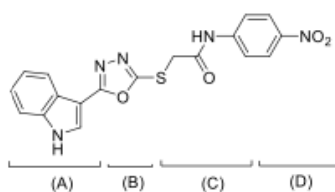
- 12; R₁ = 2,4-diOCH₃ ph
 13; R₁ = 2-CH₃ phenoxy methyl

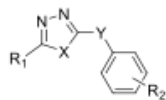


(14)

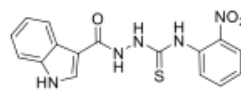


(15)

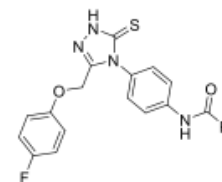




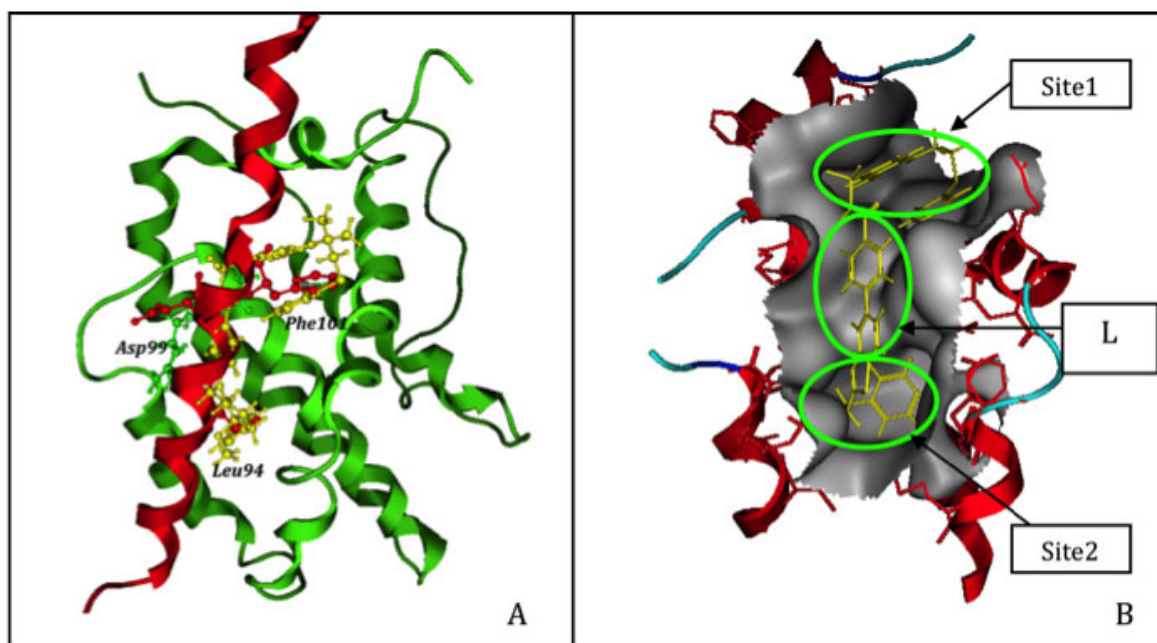
- 16a:** R₁ = 2-naphthoxy methyl, X = O, Y = S-CH₂-CONH, R₂ = 2-NO₂
16b: R₁ = 3-indolyl, X = O, Y = S-CH₂, R₂ = 3-NO₂
16c: R₁ = 3-indolyl, X = O, Y = S-CH₂, R₂ = 4-NO₂
16d: R₁ = 3-indolyl, X = O, Y = S-CH₂-CONH, R₂ = 4-NO₂
16e: R₁ = 3-indolyl, X = O, Y = S-CH₂-CONH, R₂ = 2-NO₂
16f: R₁ = 3-indolyl, X = O, Y = S-CH₂-CONH, R₂ = 4-NHCOCH₃
16g: R₁ = 3-indolyl, X = O, Y = S-CH₂-CONH, R₂ = 4-NH-CH₂-O-(2-CH₃C₆H₄)
16h: R₁ = 3-indolyl, X = N-NH₂, Y = S-CH₂-CONH, R₂ = 4-NO₂
16i: R₁ = 3-indolyl, X = N-NH₂, Y = S-CH₂-CONH, R₂ = 2-NO₂
16j: R₁ = 3-indolyl, X = O, Y = NH, R₂ = 2-NO₂
16k: R₁ = 3-indolylmethyl, X = O, Y = NH, R₂ = 3-Cl
16l: R₁ = 3-indolylmethyl, X = O, Y = NH, R₂ = 3,4-diCl
16m: R₁ = 3-indolylmethyl, X = O, Y = NH, R₂ = 4-F
16n: R₁ = 3-indolylmethyl, X = N-(4-ClC₆H₄), Y = S-CH₂-CONH, R₂ = 3,4-diCl
16o: R₁ = 3-indolylmethyl, X = N-(4-FC₆H₄), Y = S-CH₂-CONH, R₂ = 3-NO₂

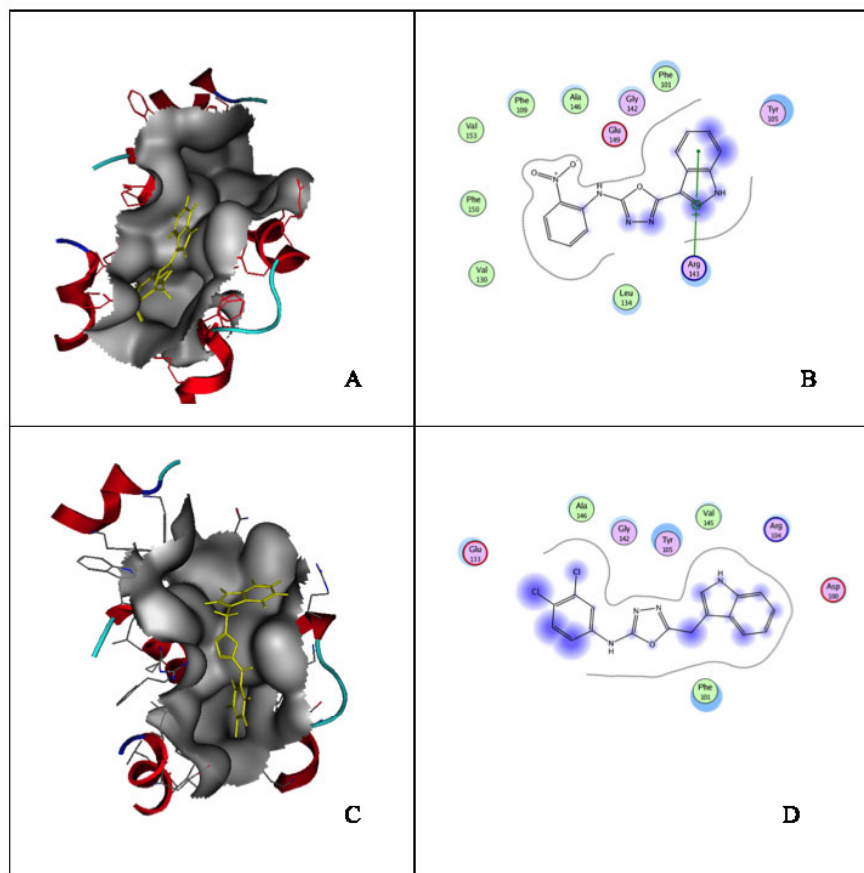


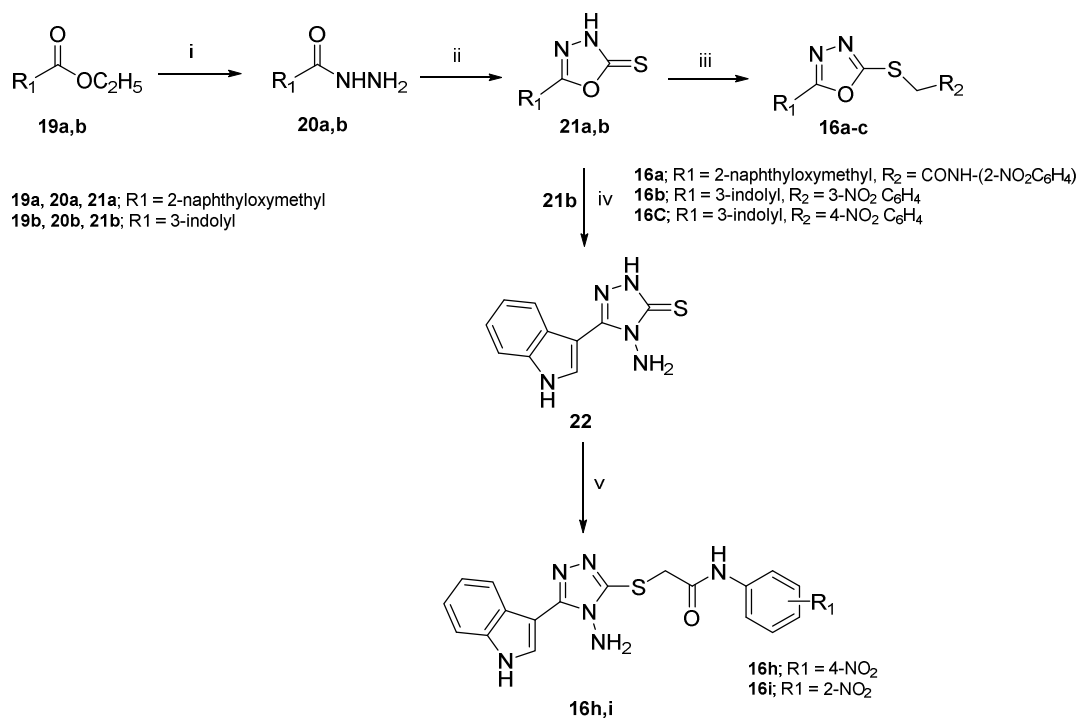
17



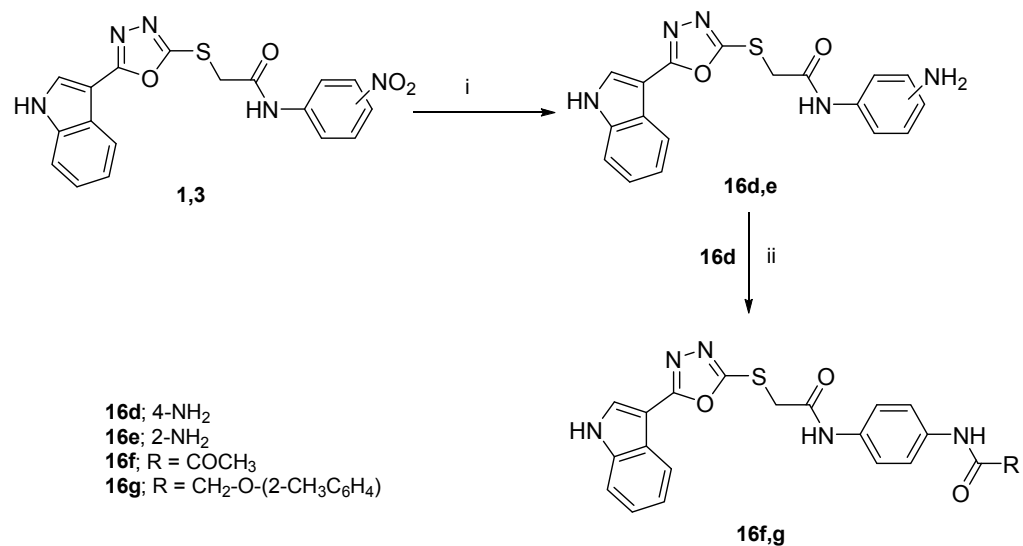
- 18a:** R = 2,4-diOCH₃ C₆H₄
18b: R = 2,4-diOH C₆H₄
18c: R = 2-methyl phenoxy methyl
18d: R = 4-[methyl-(4-methylphenylsulfonyl)amino]phenyl



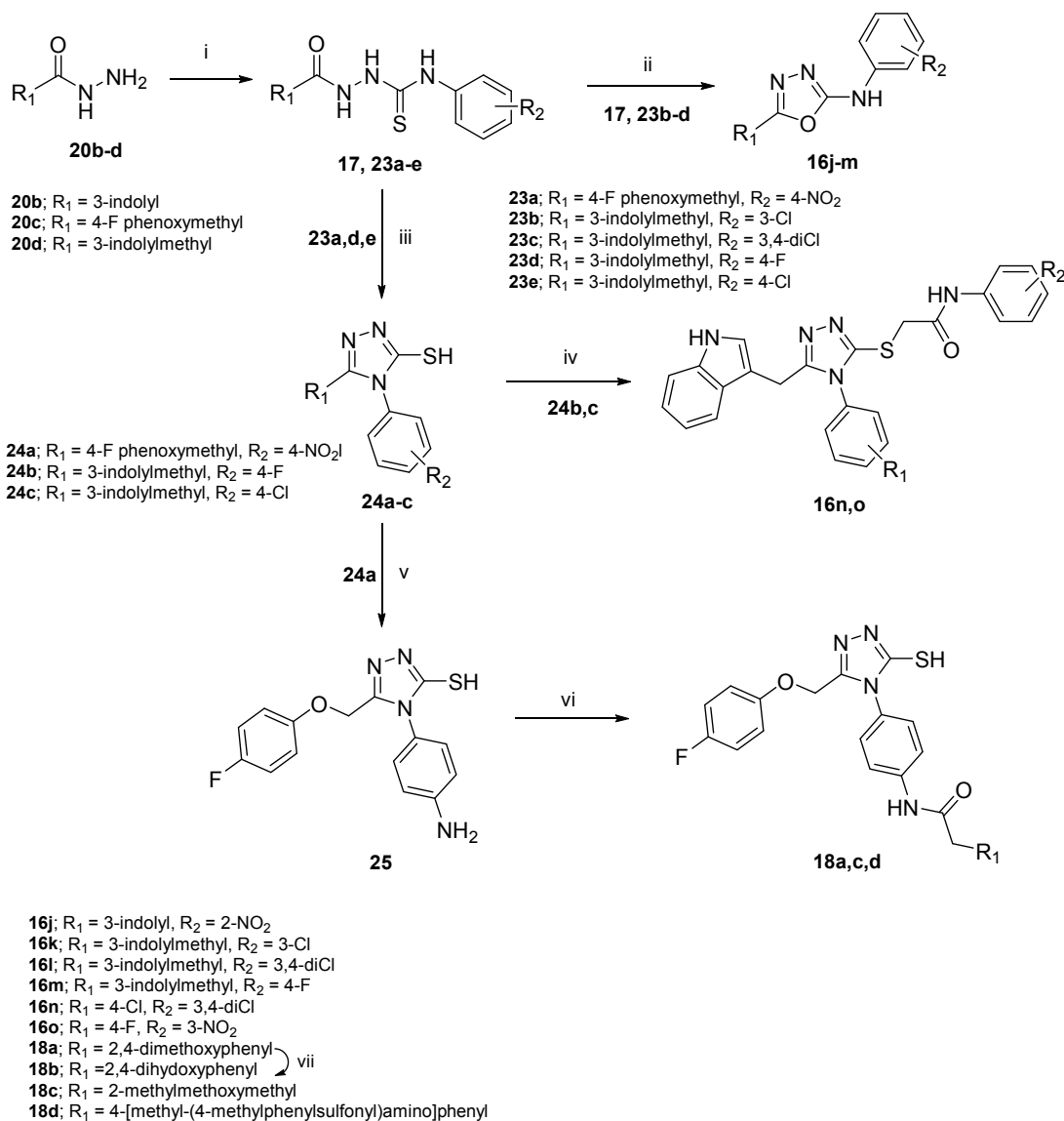




Scheme 1. Reagents and conditions: (i) N₂H₄·H₂O, ethanol, 90°C, 1 hr; (ii) a- CS₂, KOH, 80% methanol, 100°C, 12 hrs; b- H₂O, HCl; (iii) alkylchloride, NaOH, H₂O, ethanol, 90°C, 7 hrs; (iv) a- N₂H₄·H₂O 80%, reflux, 2 hrs; b- H₂O, AcOH; (v) nitrophenylchloroacetamide, NaOH, ethanol, H₂O, rt, 5 hrs.



Scheme 2. Reagents and conditions: (i) Fe, HCl, ethanol, H₂O, 100°C, 1 hr; (ii) RCOCl, THF, K₂CO₃, rt, 5 hrs



Scheme 3. Reagents and conditions: (i) substituted phenylisothiocyanate, ethanol, reflux, 1 hr; (ii) 1,3-dibromo-5,5-dimethylhydantoin, acetonitrile; (iii) a- NaOH or saturated Na₂CO₃, reflux, 3 hrs; b- HCl, H₂O; (iv) phenylacetyl bromide, KOH, 70% ethanol, rt, 12 hrs; (v) Fe, HCl, ethanol, H₂O, 90°C, 1 hr; (vi) R₂COCl, THF, K₂CO₃, rt, 4 hrs; (vii) BBr₃, DCM, 0°C, 2 hrs.